

DFTT 40/95

DTP/95/58

June 1995

The intermediate-mass \mathcal{SM} Higgs boson at the NLC: reducible and irreducible backgrounds to the Bjorken production channel¹

Stefano Moretti²

*Dipartimento di Fisica Teorica, Università di Torino,
and I.N.F.N., Sezione di Torino,
Via Pietro Giuria 1, 10125 Torino, Italy.*

*Department of Physics, University of Durham,
South Road, Durham DH1 3LE, United Kingdom.*

Abstract

Both the reducible and irreducible backgrounds to the Higgs production channel $e^+e^- \rightarrow H^0 Z^0$ at a Next Linear Collider (NLC) are studied, for the Standard Model (\mathcal{SM}) Higgs boson in the intermediate-mass range. A phenomenological analysis that does not exploit any form of tagging on the Higgs decay products is assumed.

¹Work supported in part by Ministero dell' Università e della Ricerca Scientifica.

E-mails: Moretti@to.infn.it; Stefano.Moretti@durham.ac.uk.

²Address after September 1995: Cavendish Laboratory, University of Cambridge, Madingley Road, Cambridge, CB3 0HE, U.K.

1. Introduction

The Higgs mechanism of spontaneous symmetry breaking of the electroweak interactions is a cornerstone of the Standard Model (\mathcal{SM}). It can explain why in nature some fundamental particles (i.e. leptons, quarks, the Z^0 and W^\pm gauge bosons) have a non-zero mass. A consequence of the mechanism is that it predicts the existence of a \mathcal{CP} -even neutral scalar boson (i.e. the Higgs boson H^0), which has not been observed yet. Therefore the discovery of such a particle is crucial in order to assess the correctness of the whole model.

Experimental (for the lower bound, see [1]) and theoretical (for the upper bound, see [2]) analyses have established that the Higgs boson mass should be in the range $64 \text{ GeV} \lesssim M_{H^0} \lesssim 700 \text{ GeV}$. Depending on the value of M_{H^0} , many studies on the feasibility of its detection and on the possibilities of measuring its parameters (i.e. other than the mass M_{H^0} : the width Γ_{H^0} , the spin and parity, the couplings to the other particles, etc ...) have been carried out, both for hadron [3] and e^+e^- colliders [4].

While the mass intervals $M_{H^0} \lesssim 100 \text{ GeV}$ and $M_{H^0} \gtrsim 2M_{W^\pm}$ should be easily covered by LEP II and LHC, respectively, the remaining range (intermediate-mass), which is beyond the possibilities of LEP II, appears much more difficult since for values of M_{H^0} in this interval the Higgs boson mainly decays to $b\bar{b}$ -pairs, a signature which has a huge QCD background at the LHC. Nevertheless, some important results concerning the possible detection of an intermediate-mass Higgs at the CERN pp collider have been achieved. First of all, the fact that the H^0 can decay also to Z^0Z^{0*} -pairs, in which one of the two gauge bosons is largely off-shell, allows for the Higgs detection in the ‘gold plated’ channel $H^0 \rightarrow 4\ell$ already starting from $M_{H^0} \approx 130 \text{ GeV}$. Secondly, if $M_{Z^0} \lesssim M_{H^0} \lesssim 130 \text{ GeV}$, it is possible in principle to exploit two different strategies. Either one can search for rare non-hadronic Higgs decays (i.e. $H^0 \rightarrow \gamma\gamma$), or instead detect the main decay channel (i.e. $H^0 \rightarrow b\bar{b}$) by resorting to techniques of b -flavour identification (b -tagging).

However, it should be remembered that these two latter approaches rely on the fact that a large luminosity by the CERN pp machine and/or that very high tagging efficiencies (in photon resolution and in b -tagging respectively) can be achieved by the LHC detectors. In fact, a very detailed study [5] has recently claimed that even for optimistic b -tagging performances and integrated luminosities of the order $\int \mathcal{L} dt = 10^4$

pb⁻¹, the $H^0 \rightarrow b\bar{b}$ signal cannot be cleanly extracted from the background. Nevertheless, after a few years of running at the LHC with a Center-of-Mass (CM) energy of 14 TeV, this channel might be the best way to probe the region $80 \text{ GeV} \lesssim M_{H^0} \lesssim 100 \text{ GeV}$, whereas (if a higher luminosity can be achieved) the $H^0 \rightarrow \gamma\gamma$ signature is better for $100 \text{ GeV} \lesssim M_{H^0} \lesssim 130 \text{ GeV}$.

Now, if we consider that other than in the ‘detection’ of the \mathcal{SM} Higgs boson we are interested in measuring its parameters in detail (because of, e.g. the implications that some of these could have for the existence of possible Supersymmetric extensions of the \mathcal{SM}), the importance of a Next Linear Collider (NLC) is immediately apparent. The advantage of such a machine (where two electron-positron beams linearly collide at a CM energy $\gtrsim 300\text{--}350 \text{ GeV}$) with respect to a hadron collider is that here the QCD background is drastically reduced, and one can easily exploit in the intermediate-mass range the main decay channel $H^0 \rightarrow b\bar{b}$.

For a first stage NLC (with $\sqrt{s} \approx 300\text{--}350 \text{ GeV}$) the main production mechanism of an intermediate-mass Higgs is the Bjorken reaction $e^+e^- \rightarrow Z^{0*} \rightarrow Z^0 H^0$ [6], which dominates over the $W^\pm W^\mp$ and $Z^0 Z^0$ fusion channels $e^+e^- \rightarrow \bar{\nu}_e \nu_e W^{\pm*} W^{\mp*} (e^+e^- Z^{0*} Z^{0*}) \rightarrow \bar{\nu}_e \nu_e (e^+e^-) H^0$ [7]. At larger CM energies ($\sqrt{s} \gtrsim 500 \text{ GeV}$) it is the other way round.

Because of the crucial role that a NLC could have for detecting and studying a Higgs boson with an intermediate-mass, it is then extremely important to exploit all possible search strategies and to carefully know all the corresponding backgrounds (both reducible and irreducible), which could, in principle, prevent measuring the parameters of the H^0 with the needed accuracy.

It is the purpose of this paper to study the characteristics of the signal and of all possible backgrounds for a ‘Bjorken Higgs’ in the intermediate-mass range produced at the NLC. We will one assume as a search strategy the method of calculating the mass recoiling against the Z^0 (missing-mass analysis) [8], without selecting any of the specific Higgs decay channels but instead considering them altogether in a sort of ‘inclusive’ analysis. In this kind of approach the Z^0 is most conveniently reconstructed by its e^+e^- and $\mu^+\mu^-$ decay modes, but also hadronic Z^0 decays, even the case $Z^0 \rightarrow b\bar{b}$ (with b -tagging), can be used. For our convenience, we will take in the numerical computations the Z^0 to be on-shell.

Such a strategy has the useful feature of being completely independent of assump-

tions about the H^0 decay modes but requires only tagging only the decay products of the Z^0 produced in the two-to-two body Bjorken reaction. Therefore, it demands less experimental effort, with respect to the case in which ‘exclusive’ Higgs channels are considered, whether one attempts the full kinematic reconstruction of the reaction $e^+e^- \rightarrow Z^0 H^0$ (via the decays $Z^0 H^0 \rightarrow$ jets and/or leptons), or one directly reconstructs the invariant mass from the jets (through the decays $H^0 \rightarrow b\bar{b}$ and/or $W^{\pm*}W^{\mp}$) [8].

On the contrary, in this ‘inclusive’ approach, it is necessary then not only to compute the rates for all possible decay channels of the Higgs boson and the corresponding irreducible backgrounds, but also the ones of reactions producing a Z^0 in association with additional particles faking possible Higgs decays, which appear in the invariant mass recoiling against the primary Z^0 but do not contribute to the signal spectrum. Therefore, reducible backgrounds such as, e.g. the processes $e^+e^- \rightarrow Z^0 q\bar{q}$, for light flavours $q = u, d, s, c$ should now be considered. This generally acts in the direction of reducing the significance of the signal, as the Higgs boson practically never decays to $q\bar{q}$ -light pairs, whereas the contribution from events $e^+e^- \rightarrow Z^0 Z^{0*} + Z^0 \gamma^* \rightarrow Z^0 q\bar{q}$ is expected to be quite large [8].

In general, however, the use of missing-mass techniques applied to the process $e^+e^- \rightarrow Z^0 H^0$ is quite powerful, as it provides a very efficient experimental technique to detect the Higgs scalar or to rule out this particle with certainty. Moreover, it is particularly important, e.g. in the Minimal Supersymmetric extension of the Standard Model (\mathcal{MSSM}), if $M_\chi < M_h/2$ (where χ represents a neutralino and h the lightest \mathcal{MSSM} neutral scalar boson). In fact, in this case, the ‘invisible’ decay $h \rightarrow \chi\chi$ is the dominant decay channel in the intermediate range of M_h and cannot be directly measured. Nevertheless, by missing-mass analyses, the signal $e^+e^- \rightarrow Zh \rightarrow (\ell^+\ell^-)(\chi\chi)$ ($\ell = e$ or μ) should clearly appear as a peak in the recoiling mass distribution [9].

The plan of this paper is as follows. In Section 2 we give brief details of the computations, as well as the input numerical parameters. In Section 3 we discuss the results, whereas in Section 4 we present the conclusions.

2. Calculation

We are interested in an analysis that does not perform any tagging on the decay products of a \mathcal{SM} Higgs boson produced via the Bjorken bremsstrahlung reaction $e^+e^- \rightarrow H^0 Z^0$. We shall focus on the intermediate-mass range $M_{Z^0} \lesssim M_{H^0} \lesssim 2M_{W^\pm}$, where the quantitatively significant Higgs decay channels are into $b\bar{b}$ -, $W^{\pm*}W^\mp$ - and $Z^{0*}Z^0$ -pairs, giving the signatures jj (no flavour identification of b -quarks is assumed in our analysis), jjW^\mp , $\ell\nu_\ell W^\mp$, jjZ^0 , $\ell\bar{\ell}Z^0$ and $\nu_\ell\bar{\nu}_\ell Z^0$, with all possible subsequent decays of the on-shell gauge bosons. Thus we are forced to study the complete processes

$$e^+e^- \rightarrow f\bar{f}Z^0, \quad (1)$$

$$e^+e^- \rightarrow f\bar{f}'W^\pm Z^0, \quad (2)$$

$$e^+e^- \rightarrow f\bar{f}Z^0 Z^0, \quad (3)$$

($f = \ell, \nu_\ell$ and q , with $\ell = e, \mu, \tau$ and $q = u, d, s, c, b$). These include at tree-level all the relevant (both reducible and irreducible) backgrounds to the Bjorken reaction, followed by the Higgs decay into the above channels. For simplicity, and since the final results would not significantly change, we neglect here the case of the H^0 decaying into gg -pairs through loops of heavy quarks and of the non-resonant diagrams entering into the processes $e^+e^- \rightarrow Z^0 + n$ jets (with $n \geq 2$), which are at least $\mathcal{O}(\alpha_W^3 \alpha_s^2)$ suppressed (i.e. a factor of $\alpha_W \alpha_s^2$ if compared to the $Z^0 H^0$ signal, especially if all the jets are very well separated). In addition, Higgs decays into $\gamma\gamma$ and $Z^0\gamma$ can be safely neglected, since they contribute only at the level $\mathcal{O}(10^{-3})$. At the same time, it is not necessary to compute their backgrounds in $e^+e^- \rightarrow Z^0\gamma\gamma$ and $e^+e^- \rightarrow Z^0 Z^0\gamma$ events, if one asks that the mass recoiling against the Z^0 does not contain very hard photons.

Concerning possible backgrounds arising from the $e^+e^- \rightarrow t\bar{t} \rightarrow b\bar{b}W^+W^-$ top-pairs production and decay, these should be drastically suppressed if we assume for the top mass a value $m_t \gtrsim 175$ GeV [10] and to tag $Z^0 \rightarrow \ell^+\ell^-$ (with $\ell = e$ or μ). In fact, at $\sqrt{s} = 300$ GeV the $t\bar{t}$ -threshold is far away, whereas at $\sqrt{s} = 500$ GeV, if one takes, e.g. $m_t = 180$ GeV, then the total rate is only $\approx \sigma(e^+e^- \rightarrow t\bar{t}) \times [BR(W \rightarrow \ell\nu_\ell)]^2 \approx 7$ fb [11]. If $Z^0 \rightarrow jj$ or $b\bar{b}$ (with b -tagging), the $t\bar{t}$ background would deserve a more detailed treatment that we are not performing here. However, we expect even this case to be manageable, e.g. by exploiting the fact that the Z^0 produced via the two-body Bjorken reaction is ‘practically’ mono-energetic (with $E_{Z^0} \approx E_{\text{ave}} = (s - M_{H^0}^2 + M_{Z^0}^2)/2\sqrt{s}$).

In fact, this is true apart from photon bremsstrahlungs off e^+e^- -lines (i.e. Initial State Radiation, ISR). Nevertheless, since the mean e^+e^- CM energy loss $\delta_{\sqrt{s}}$ due to ISR is, e.g. $\approx 5\%$ at $\sqrt{s} = 500$ GeV [12], one can choose a window wide enough ($\approx \delta_{\sqrt{s}} \times \sqrt{s}$) to prevent complications due to such effects³. Therefore we expect the cut, say, $|E_{Z^0} - E_{\text{ave}}| < 12.5$ GeV to be quite efficient in reducing the numbers of $t\bar{t}$ events around the H^0 -peak, as it has been demonstrated in a similar context in ref. [13]. In addition, and contemporaneously, one can always require that $M_{jj(b\bar{b})} \approx M_{Z^0}$, in order to enforce the above E_{Z^0} cut, improving the mass resolution as much as needed, depending on the size of the energy losses by ISR⁴. For these reasons we do not study here, among the background processes, the $t\bar{t}$ -production and decay.

Both the QED radiative corrections and the genuine weak ones to the Bjorken process have been computed [15]. However, since the backgrounds evaluated here are at tree-level, for consistency, we use the lowest order rates. In addition, these corrections are known to be well under control.

To give an idea of the complexity of the computations, we show in fig. 1a-c all the Feynman diagrams describing at tree-level processes (1)–(3) respectively, for $f^{(\prime)} \neq \nu_e, e$. The cases $f^{(\prime)} = \nu_e, e$ are even more complicated, since they include also diagrams in which the incoming electron/positron lines are directly connected to the final states, and are not shown here. The matrix elements for the three above reactions have been computed using the method of ref. [16], the FORTRAN codes we have written and optimised have been checked for BRS invariance [17] and compared to the corresponding MadGraph/HELAS outputs [18].

In order to keep the interplay between the various resonances, which appear in the integration domains of the final states in (1)–(3) when all tree-level contributions are kept into account, under control, we have adopted the technique [11, 13] of splitting the corresponding Feynman amplitudes squared into a sum of different (non-gauge-invariant) terms and then integrating each according to its resonant structure. We will not discuss this in any detail, instead we refer the reader to the cited papers.

³The inclusion of Linac energy spread and beamsstrahlung should not drastically change this strategy, at least for the ‘narrow’ D–D and TESLA collider designs (see ref. [12]).

⁴We would also like to stress here how this procedure should make it unnecessary to use the veto $M_{jj(b\bar{b})j} \neq m_t$ suggested in ref. [14], which would imply tagging three particles, thus spoiling the attractiveness of this analysis (which only requires tagging the two decay products of the ‘Bjorken Z^0 ’).

Here, we only want to stress that the ‘Bjorken diagrams’ giving the signals are the numbers 5 in fig. 1a, 29 in fig. 1b and 18 in fig. 1c⁵, and that when in the next section we speak of the ‘missing-mass distribution’ we mean the sum of the differential cross sections corresponding to the three processes, each of which is obtained by summing together the non-gauge-invariant ‘cross sections’. In that way, the invariance is perfectly recovered in the end [11, 13]. Obviously, the three above processes do not interfere at all, and they are computed separately.

The multi-dimensional integrations over the phase spaces have been performed numerically using VEGAS [19]. The following values of the parameters have been adopted: $M_{Z^0} = 91.1$ GeV, $\Gamma_{Z^0} = 2.5$ GeV, $M_{W^\pm} \equiv M_{Z^0} \cos(\theta_W) \approx 80$ GeV, $\Gamma_{W^\pm} = 2.2$ GeV, and $\sin^2(\theta_W) = 0.23$. For the fermions: $m_\mu = 0.105$ GeV, $m_\tau = 1.78$ GeV, $m_s = 0.3$ GeV, $m_c = 1.4$ GeV, $m_b = 4.25$ GeV. All neutrinos and the first generation of quarks/leptons has been considered massless: i.e. $m_{\nu_e} = m_{\nu_\mu} = m_{\nu_\tau} = m_e = m_u = m_d = 0$. The electromagnetic coupling constant has been set equal to $1/128$. For the Higgs width (i.e. Γ_{H^0}) we have adopted the tree-level expression corrected for the running of the quark masses in the vertices $H^0 q\bar{q}$ (for $q = s, c$ and b). They have been evaluated at the scale $\mu = M_{H^0}$ [20]. Therefore, in order to be consistent we have used the same running masses in the corresponding vertex of the production processes here considered. Finally, we have avoided adopting any form of Narrow Width Approximation (NWA), i.e. the procedure of separately computing the on-shell production times the branching fractions, into the final state of processes (1)–(3), of the various intermediate particles appearing in the diagrams of figs. 1-3. Only the final state Z^0 ’s and W^\pm ’s are considered on-shell, as for them we have included neither the effects of their finite width nor those of their decays. Also, the ISR [12] was not included. However, we are confident that properly keeping into account all these aspects would not affect our conclusions.

⁵Even though also the graphs number 27, 28 (11, 12) in fig. 1b(c), and 17 in fig. 1c are namely Higgs ‘Bjorken diagrams’, in this case the H^0 goes either into $f\bar{f}$ -pairs, followed by W^\pm/Z^0 -bremsstrahlung, or into on-shell $Z^0 Z^0$ -pairs: decays that are strongly suppressed or that take place above the range we are interested in here respectively. However, the first kind of graphs (i.e. with W^\pm/Z^0 -bremsstrahlung) are properly included in the $H^0 \rightarrow f\bar{f}'W^\pm(f\bar{f}'Z^0)$ resonance (see ref. [13] for more details).

3. Results

A careful study concerning intermediate-mass Higgs searches at 300–500 e^+e^- linear colliders, for a H^0 produced via the Bjorken process, including also a missing-mass analysis when no assumption on the Higgs decay modes is done, was presented in ref. [8]. In that paper, only the $e^+e^- \rightarrow Z^0Z^0$ background was considered. More recently, a few works studying ‘exclusive’ signals (i.e. when the decay channels of the Higgs boson are separately considered), and corresponding backgrounds, have been completed. Ref. [21] studied the channels $H^0Z^0 \rightarrow (b\bar{b})(\mu^+\mu^-)$, $(W^\pm W^\mp)(\mu^+\mu^-)$, $(Z^0Z^{0*})(\mu^+\mu^-)$, and the backgrounds $e^+e^- \rightarrow Z^0Z^{0*}$, $Z^0\gamma^*$, $\gamma^*\gamma^*$, $Z^0W^\pm W^\mp$, $Z^0Z^0Z^{0*}$, in the intermediate mass range. For the case $e^+e^- \rightarrow e^+e^-H^0 \rightarrow e^+e^-b\bar{b}$, see ref. [22]. While ref. [14] contains a very complete analysis of various ‘exclusive’ signals and backgrounds over the whole allowed range of M_{H^0} . This study is based on the complete tree-level computation of the processes $e^+e^- \rightarrow \ell^+\ell^-b\bar{b}$ (with $\ell = e$ or μ) and $e^+e^- \rightarrow \ell_1\ell_2V_1V_2$ (where ℓ_1, ℓ_2 represent e - and μ -leptons and neutrinos, whereas V_1V_2 indicate the massive electroweak gauge bosons W^\pm and Z^0).

Our results are presented in tab. I and in figs. 2-4. In order to keep all our matrix elements safe from singularities we have implemented the following cuts: $M_{f\bar{f}'(\prime)} > 10$ GeV for all flavours $f^{(\prime)}$, plus $|\cos\theta_{e,\nu_e}| < 0.95$ and $E_{e,\nu_e} > 10$ GeV for electrons/positrons and corresponding neutrinos. These cuts shouldn’t affect the consistency of the analysis since, on the one hand, the invariant mass $M_{f\bar{f}'(\prime)}$ for the signals is always $\approx M_{H^0}$, M_{W^\pm} or M_{Z^0} and, on the other hand, the region along the beam pipe and the one with soft energy are naturally restricted by the requirements of the detectors.

Fig. 2 shows the distribution in missing-mass $d\sigma/dM_{\text{miss}}$, where $M_{\text{miss}}^2 = [(p_{e^+} + p_{e^-}) - p_{Z^0}]^2$, for processes (1)–(3) summed together, for the selection of Higgs masses $M_{H^0} = 110, 125, 140$ and 155 GeV, at the CM energies $\sqrt{s} = 300$ and 500 GeV. We have not included here any BR for the massive vector boson Z^0 . It is clear from these plots that the prospects of disentangling the Higgs boson in the mass range $110 \text{ GeV} \lesssim M_{H^0} \lesssim 155 \text{ GeV}$ remain quite promising even in the presence of all the backgrounds coming from the non Higgs resonant diagrams of processes (2)–(3), summed over all ℓ - and q -flavour combinations, if a mass resolution of ≈ 15 GeV or better can be achieved (bins in fig. 2 are 5 GeV wide).

In process (2) the background is relevant in the M_{miss} spectrum only for $M_{f\bar{f}'W^\pm} \gtrsim$

$2M_{W^\pm} \approx 160$ GeV, since here the main contribution comes from the triple vector boson production $Z^0 W^\pm W^{\mp*}$ (with the subsequent decay $W^{\pm*} \rightarrow f\bar{f}'$, diagrams # 7–9, 18–20, 23–26 of fig. 1b). Therefore, in $e^+e^- \rightarrow f\bar{f}'W^\pm Z^0$ both the diagrams containing $Z^0 Z^{0*}$ production diagrams (followed by $Z^{0*} \rightarrow f\bar{f}$ with a successive W^\pm -bremsstrahlung, graphs # 12–15 with Z^0 propagator, or by $Z^{0*} \rightarrow W^\pm W^{\mp*} \rightarrow W^\pm f\bar{f}'$, diagrams # 23–24 in fig. 1b) and the non resonant diagrams (# 1–6, 10–11, 12–15 with γ propagator, 16–17 and 21–22 of fig. 1b), as well all the interferences, are negligible. For process (3) the shape is rather flat in the region $M_{H^0} \gtrsim 110$ GeV, with the main contribution here coming from $Z^0 Z^0 \gamma^*$ production (followed by $\gamma^* \rightarrow f\bar{f}$, graphs # 4–6 with γ propagator, in fig. 1c), whereas all the other background contributions (i.e. the $Z^{0*} \rightarrow f\bar{f}$ resonant diagrams # 4–6 with Z^0 propagator, and the $H^0 \rightarrow f\bar{f}[Z^0 Z^0]$ graphs # 13–14[15–17], as well all the interferences) are quite small. Since for processes (2) and (3) the quantity M_{miss} has a natural minimum at M_{W^\pm} and M_{Z^0} , respectively, we cannot properly consider here the case of the Higgs peak overlapping with the Z^0 one (i.e. $M_{H^0} \approx 90$ GeV). To do this, we should consider five particle final states (with the substitutions $W^\pm \leftrightarrow f\bar{f}'$ and $Z^0 \leftrightarrow f\bar{f}$ in (2)–(3)), which are beyond our intentions. From these two processes, however, we expect completely negligible rates in the Z^0 -region (see the rapidly falling shape of the distribution at small values of M_{miss} , especially at $\sqrt{s} = 500$ GeV, in fig. 2). Process (1), especially important in the case $M_{H^0} \approx M_{Z^0}$, has been carefully studied in ref. [8], and we do not repeat here the same discussion.

The strength of the couplings of the H^0 to the Z^0 and to the W^\pm can be deduced by the magnitude of the cross sections (in the bremsstrahlung and fusion processes), whereas the ones to (some of) the fermions are measurable (at least relative to, e.g. $b\bar{b}$) through the BRs, by singularly selecting the various Higgs decay channels [21]. If one would like to verify the expected spin and parity of the \mathcal{SM} Higgs boson then he should turn to study, e.g. the spectrum of the cosine of the angle of the Z^0 with respect to the beam direction, i.e. $\cos\theta_Z$. We know that in the case of production of a scalar boson in association with a vector boson, the distribution in this angle tends to approach the $\sin^2\theta_Z$ law at high energies [21, 23]. However, since the Bjorken Higgs contribution is quite small if compared to the total sample of events (1)–(3) (see tab. I), this dependence is almost completely washed out. In fact, fig. 3 shows that the main contribution is due to the $e^+e^- \rightarrow f\bar{f}'Z^0$ process through $Z^0 Z^0$ -production, which has

the largest cross section. The shape is peaked in the very forward region, reflecting the t -channel exchange of a fermion.

However, suitable cuts in M_{miss} around M_{H^0} (e.g. $|M_{\text{miss}} - M_{H^0}| < 15$ GeV) and in E_{Z^0} around E_{ave} (e.g. $|E_{Z^0} - E_{\text{ave}}| < 12.5$ GeV) get rid of the most part of the backgrounds, practically keeping all the signals. Fig. 4 shows the dependence of the inclusive cross section on $\cos \theta_Z$ once the above cuts in M_{miss} and E_{Z^0} are implemented. The $\sin^2 \theta_Z$ law stands out now quite clearly, especially in the central region of the spectrum and for $\sqrt{s} = 500$ GeV. At $\sqrt{s} = 300$ GeV the backgrounds are still quite effective. From fig. 4 it is however clear that a cut in the angle of the Z^0 -direction with respect to the beam, say, $|\cos \theta_Z| < 0.8$, should be quite successful in improving the signal-to-noise ratio, thus allowing for high precision measurements of the Higgs boson parameters.

4. Conclusions

In summary, we have computed at tree-level integrated and differential rates for the reactions $e^+e^- \rightarrow f\bar{f}Z^0$, $e^+e^- \rightarrow f\bar{f}'W^\pm Z^0$ and $e^+e^- \rightarrow f\bar{f}Z^0Z^0$ at NLC CM energies ($\sqrt{s} = 300, 500$ GeV), for all possible combinations of flavours $f^{(\prime)} = u, d, s, c, b, e, \nu_e, \mu, \nu_\mu, \tau, \nu_\tau$. These processes involve the production of the \mathcal{SM} Higgs boson H^0 through the Bjorken channel $e^+e^- \rightarrow H^0Z^0$, followed by $H^0 \rightarrow b\bar{b}$, $H^0 \rightarrow W^\pm W^\mp \rightarrow W^\pm f\bar{f}'$ and $H^0 \rightarrow Z^0Z^{0*} \rightarrow Z^0f\bar{f}$, respectively (the main Higgs decay channels in the intermediate mass range), and the corresponding (both reducible and irreducible) backgrounds. In particular, we focused our attention on the interval $110 \text{ GeV} \lesssim M_{H^0} \lesssim 155 \text{ GeV}$. It is extremely important for these mass values to exploit all the possible Higgs search strategies and to know all the corresponding backgrounds, since it is not clear whether the intermediate mass range can be successfully covered by the LHC, and at the same time it is beyond the possibilities of LEP II. In this study we have assumed an ‘inclusive’ analysis in missing-mass, which does not exploit any form of tagging on the H^0 -decay products but only on the ones of the Z^0 produced in the Bjorken bremsstrahlung reaction. Although definite numerical results can be given only after a proper experimental simulation (including kinematical cuts, detector efficiencies, hadronization, etc ...), we conclude that, via such analysis, Higgs signals from the Bjorken channel should be clearly detectable for reasonable mass and energy

resolutions, and studies of the properties of the H^0 should be feasible, already for the standard integrated luminosity of 10 fb^{-1} per year, particularly at $\sqrt{s} = 500 \text{ GeV}$.

Acknowledgments

We are grateful to A.G. Akeroyd for useful comments and for reading the manuscript.

References

- [1] P. Janot, Talk delivered at the *First General Meeting of the LEP II Workshop*, CERN, Geneva, Switzerland, 2–3 February 1995.
- [2] M. Veltman, *Phys. Lett.* **B70** (1977) 253;
B.W. Lee, C. Quigg and G.B. Thacker, *Phys. Rev. Lett.* **38** (1977) 883; *Phys. Rev.* **D16** (1977) 1519.
- [3] Proc. of the “*Large Hadron Collider Workshop*”, Aachen, 4-9 October 1990, eds. G. Jarlskog and D. Rein, Report CERN 90-10, ECFA 90-133, Geneva, 1990;
J.F. Gunion and T. Han, *preprint* UCD-94-10, April 1994.
- [4] Proc. of the ECFA workshop on LEP 200, A. Bohm and W. Hoogland eds., Aachen FRG, 29 Sept.-1 Oct. 1986, CERN 87-08;
Proceedings of the Workshop “*Physics and Experiments with Linear Colliders*”, Saariselkä, Finland, 9-14 September 1991, eds. R. Orawa, P. Eerola and M. Nordberg, World Scientific Publishing, Singapore, 1992;
Proc. of the Workshop “ *e^+e^- Collisions at 500 GeV. The Physics Potential*”, Munich, Annecy, Hamburg, 3-4 February 1991, ed. P.M. Zerwas, DESY pub. 92-123A/B, August 1992; DESY pub. 93-123C, December 1993;
Proc. of the ECFA workshop on “ *e^+e^- Linear Colliders LC92*”, R. Settles ed., Garmisch Partenkirchen, 25 July-2 Aug. 1992, MPI-PhE/93-14, ECFA 93-154;
Proc. of the I-IV Workshops on Japan Linear Collider (JLC), KEK 1989, 1990, 1992, 1994, KEK-Reports 90-2, 91-10, 92-1, 94-1.
- [5] D. Froidevaux, E. Richter-Was, *preprint* CERN-TH.7459/94, September 1994.

- [6] J.D. Bjorken, Proceedings of the “*Summer Institute on Particle Physics*”, *SLAC Report* 198 (1976);
 B.W. Lee, C. Quigg and H.B. Thacker, *Phys. Rev.* **D16** (1977) 1519;
 J. Ellis, M.K. Gaillard and D.V. Nanopoulos, *Nucl. Phys.* **B106** (1976) 292;
 B.L. Ioffe and V.A. Khoze, *Sov. J. Part. Nucl.* **9** (1978) 50.
- [7] D.R.T. Jones and S.T. Petkov, *Phys. Lett.* **B84** (1979) 440;
 R.N. Chan and S. Dawson, *Phys. Lett.* **B136** (1984) 196;
 K. Hikasa, *Phys. Lett.* **B164** (1985) 341;
 G. Altarelli, B. Mele and F. Pitolli, *Nucl. Phys.* **B287** (1987) 205.
- [8] P. Grosse-Wiesmann, D. Haidt and H.J. Schreiber, in Proc. of the Workshop “ *e^+e^- Collisions at 500 GeV. The Physics Potential*”.
- [9] P. Janot, in Proc. of the Workshop “ *e^+e^- Collisions at 500 GeV. The Physics Potential*” (part A/B).
- [10] CDF Collaboration, *preprint* FERMILAB-PUB-95-022-E, CDF-PUB-TOP-PUBLIC-3040, March 1995;
 D0 Collaboration, *preprint* FERMILAB-PUB-95-028-E, March 1995.
- [11] A. Ballestrero, E. Maina and S. Moretti, *Phys. Lett.* **B335** (1994) 460.
- [12] T. Barklow, P. Chen and W. Kozanecki, in Proc. of the Workshop “ *e^+e^- Collisions at 500 GeV. The Physics Potential*” (part A/B).
- [13] S. Moretti, *U. of Torino preprint* DFTT 69/94, *Durham U. preprint* DTP/95/02, December 1994.
- [14] V. Barger, K. Cheung, A. Djouadi, B.A. Kniehl, R.J.N. Phillips and P.M. Zerwas, in Proc. of the Workshop “ *e^+e^- Collisions at 500 GeV. The Physics Potential*” (part C).
- [15] J. Fleischer and F. Jegerlehner, *Nucl. Phys.* **B216** (1983) 469;
 A. Denner, J. Kublbeck, R. Mertig and M. Bohm, *Z. Phys.* **C56** (1992) 261;
 B.A. Kniehl, *Z. Phys.* **C55** (1992) 605;
 J. Fujimoto, Y. Kurihara and Y. Shimizu, in Proc. of the IV Workshop on Japan Linear Collider.

- [16] K. Hagiwara and D. Zeppenfeld, *Nucl. Phys.* **B274** (1986) 1.
- [17] K. Fujikawa, B.W. Lee and A.I. Sanda, *Phys. Rev.* **D6** (1972) 2923;
 C. Becchi, A. Rouet and B. Stora, *Comm. Math. Phys.* **42** (1975) 127; *Ann. Phys.* **98** (1976) 287;
 B.W. Lee, C. Quigg and H.B. Thacker, *Phys. Rev* **D16** (1977) 1519;
 M.S. Chanowitz and M.K. Gaillard, *Nucl. Phys.* **B261** (1985) 379;
 G.J. Gounaris, R. Kögerler and H. Neufeld, *Phys. Rev.* **D34** (1986) 3257.
- [18] T. Stelzer and W.F. Long, *Comp. Phys. Comm.* **81** (1994) 357;
 E. Murayama, I. Watanabe and K. Hagiwara, HELAS: HELicity Amplitude Sub-routines for Feynman Diagram Evaluations, *KEK Report* 91-11, January 1992.
- [19] G.P. Lepage, *Jour. Comp. Phys.* **27** (1978) 192.
- [20] E. Braaten and J.P. Leveille, *Phys. Rev.* **D22** (1980) 715;
 N. Sakai, *Phys. Rev.* **D22** (1980) 2220;
 T. Inami and T. Kubota, *Nucl. Phys.* **B179** (1981) 171;
 M. Drees and K. Hikasa, *Phys. Lett.* **B240** (1990) 455;
 S.G. Gorishny, A.L. Kataev, S.A. Larin and L.R. Surguladze, *Mod. Phys. Lett.* **A5** (1990) 2703;
 L.R. Surguladze, *Phys. Lett.* **B341** (1994) 60.
- [21] V. Barger, K. Cheung, A. Djouadi, B.A. Kniehl and P.M. Zerwas, *Phys. Rev.* **D49** (1994) 79.
- [22] E. Boos, M. Sachwitz, H.J. Schreiber and S. Shichanin, *Z. Phys.* **C64** (1994) 391.
- [23] Z. Kunszt and W.J. Stirling, *Phys. Lett.* **B242** (1990) 507;
 N. Brown, *Z. Phys.* **C49** (1991) 657;
 V. Barger and K. Whisnant, *Phys. Rev.* **D43** (1991) 1443;
 M.L. Stong, *preprint* TTP-95-16, April 1995.

Table Captions

table I Cross sections for the signal ($e^+e^- \rightarrow H^0 Z^0 \rightarrow X Z^0$) and for the complete processes (1)–(3) ($e^+e^- \rightarrow X Z^0$), these latter summed together, and with/without cut in M_{miss} , for $M_{H^0} = 110, 125, 140, 155$ GeV, at $\sqrt{s} = 300$ and 500 GeV. The sum over all possible combinations of flavours in eqs. (1)–(3) is implied. The underlying cuts $M_{f\bar{f}'} \geq 10$ GeV, $|\cos\theta_{e,\nu_e}| < 0.95$ and $E_{e,\nu_e} > 10$ GeV are implemented. The BR of the reconstructed Z^0 is not included.

Figure Captions

figure 1 Feynman diagrams contributing at lowest order to the processes $e^+e^- \rightarrow f\bar{f}Z^0$ (a), $e^+e^- \rightarrow D\bar{U}W^+Z^0$ (b) and $e^+e^- \rightarrow f\bar{f}Z^0Z^0$ (c), where $(D, \bar{U}) = (d, \bar{u}), (s, \bar{c}), (\mu, \bar{\nu}_\mu), (\tau, \bar{\nu}_\tau)$ and $f = u, d, s, c, b, \mu, \tau, \nu_\mu, \nu_\tau$. The diagrams for $e^+e^- \rightarrow U\bar{D}W^-Z^0$ are not shown, but they can be trivially obtained from the $U\bar{D}W^-Z^0$ ones. Internal wavy lines represent a γ , a Z^0 or a W^\pm , as appropriate. Internal dashed lines represent the Higgs boson.

figure 2 The differential distribution in missing-mass $d\sigma/dM_{\text{miss}}$, for processes (1)–(3) summed together (for all the possible combination of flavours f and f'), for $M_{H^0} = 110$ GeV (continuous line), $M_{H^0} = 125$ GeV (dashed line), $M_{H^0} = 140$ GeV (dotted line), $M_{H^0} = 155$ GeV (chain-dotted line), at $\sqrt{s} = 300$ and 500 GeV. The underlying cuts $M_{f\bar{f}'} \geq 10$ GeV, $|\cos\theta_{e,\nu_e}| < 0.95$ and $E_{e,\nu_e} > 10$ GeV are implemented. The BR of the reconstructed Z^0 is not included.

figure 3 The differential distribution in the cosine of the angle of the Z^0 with respect to the beam direction $\cos\theta_Z$, for processes (1)–(3) summed together (for all the possible combination of flavours f and f'), for $M_{H^0} = 110$ GeV (continuous line), $M_{H^0} = 125$ GeV (dashed line), $M_{H^0} = 140$ GeV (dotted line), $M_{H^0} = 155$ GeV (chain-dotted line), at $\sqrt{s} = 300$ and 500 GeV. The underlying cuts $M_{f\bar{f}'} \geq 10$ GeV, $|\cos\theta_{e,\nu_e}| < 0.95$ and $E_{e,\nu_e} > 10$ GeV are implemented. The BR of the reconstructed Z^0 is not included.

figure 4 Same as fig. 3, after the cuts $|M_{\text{miss}} - M_{H^0}| < 15$ GeV and $|E_{Z^0} - E_{\text{ave}}| < 12.5$ GeV.

σ (fb)			
M_{H^0} (GeV)	$e^+e^- \rightarrow H^0 Z^0 \rightarrow X Z^0$	$e^+e^- \rightarrow X Z^0$	$e^+e^- \rightarrow X Z^0$
$\sqrt{s} = 300(500)$ GeV			
110	204(59)	2154(1397)	65(25)
125	184(58)	2131(1394)	35(15)
140	163(56)	2116(1394)	31(12)
155	140(54)	2101(1407)	30(11)
	no M_{miss} cut	no M_{miss} cut	$ M_{\text{miss}} - M_{H^0} < 15$ GeV
$M_{f\bar{f}(\prime)} \geq 10$ GeV		$ \cos \theta_{e,\nu_e} < 0.95$	$E_{e,\nu_e} > 10$ GeV

Table I

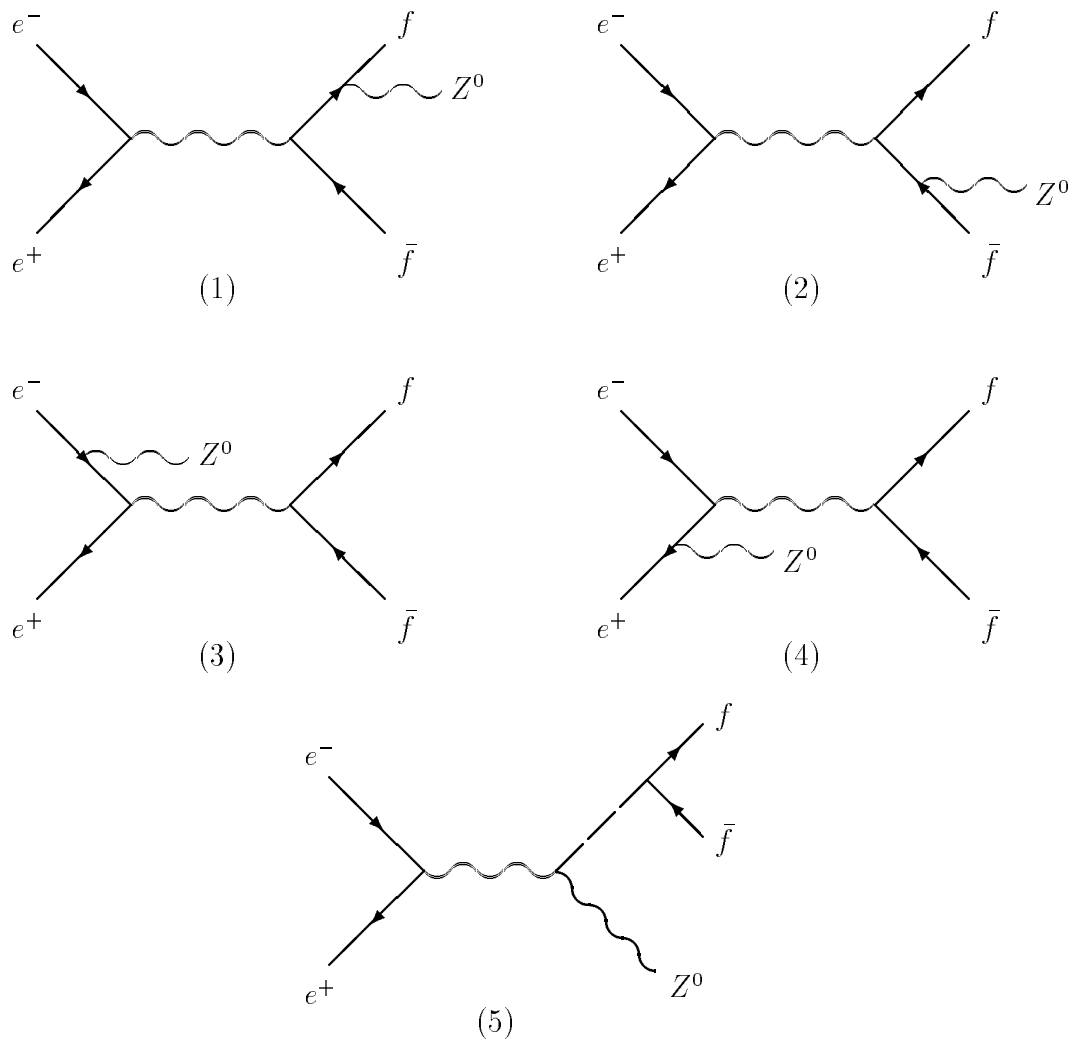


Fig. 1a

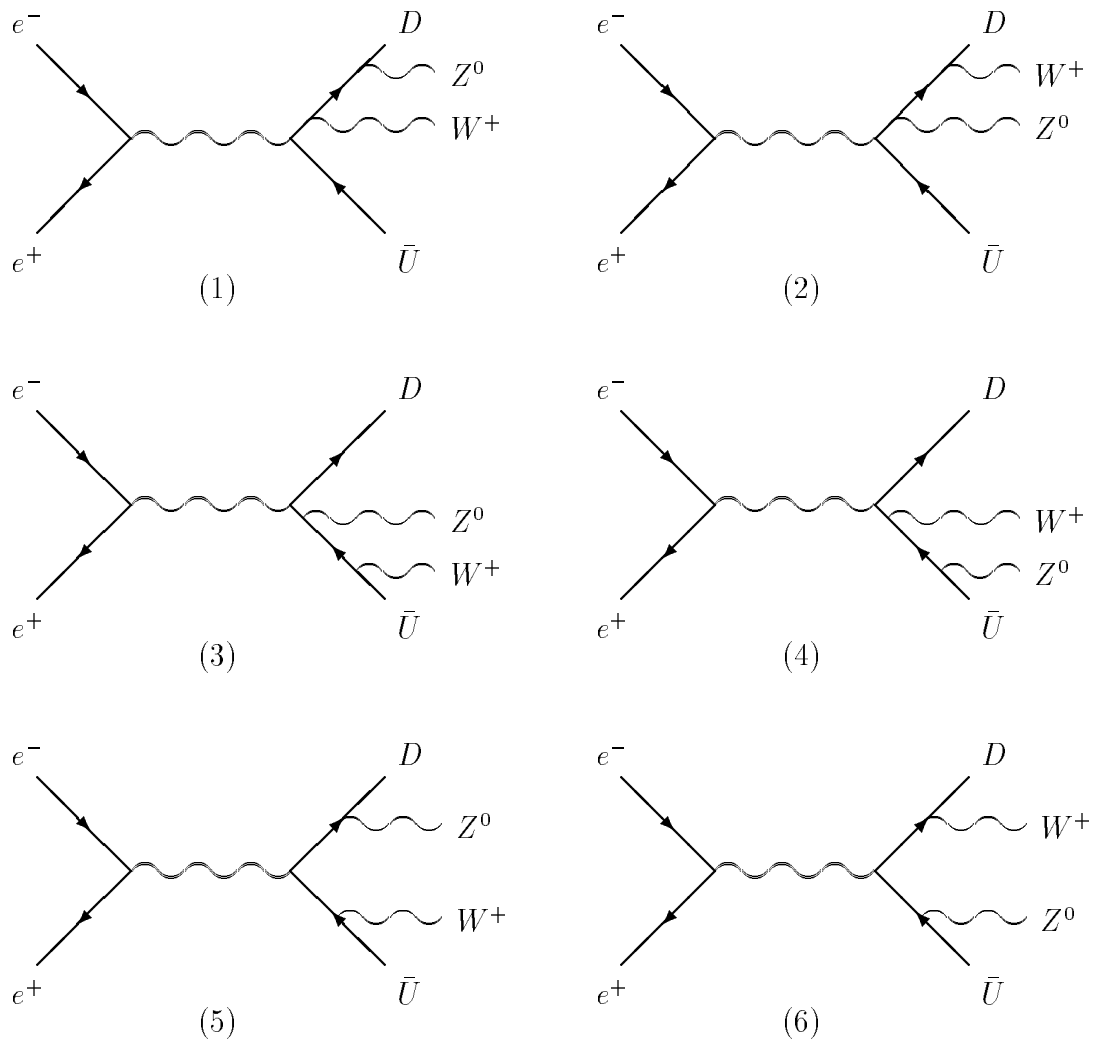


Fig. 1b

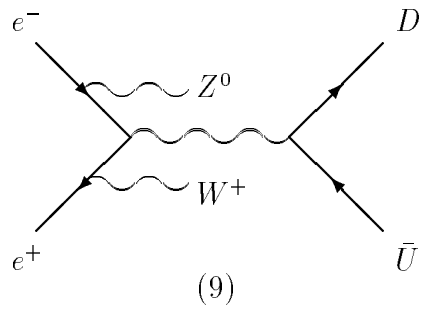
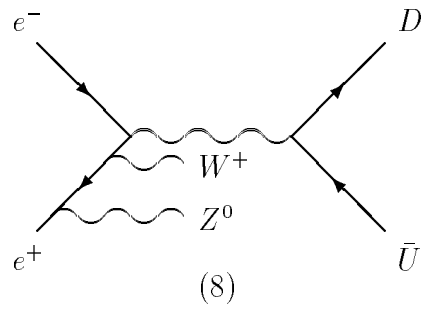
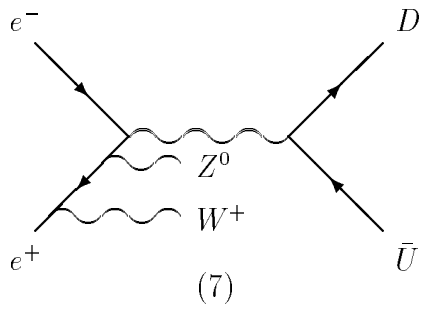


Fig. 1b (Continued)

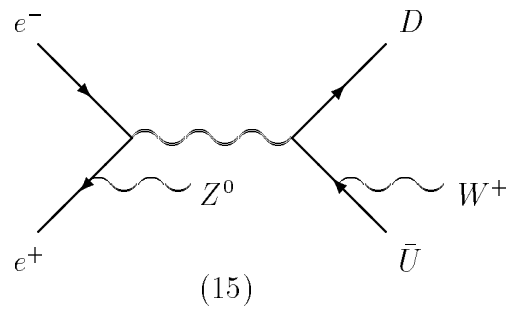
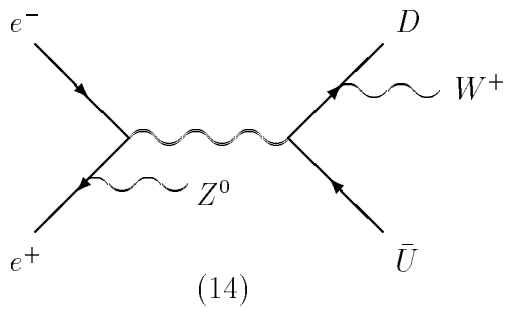
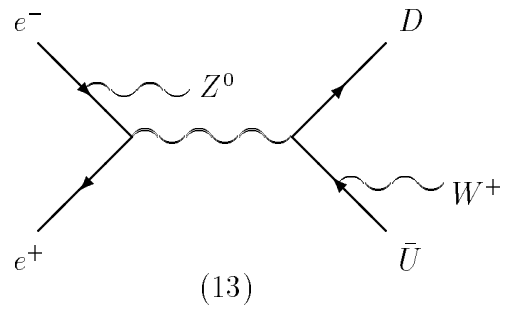
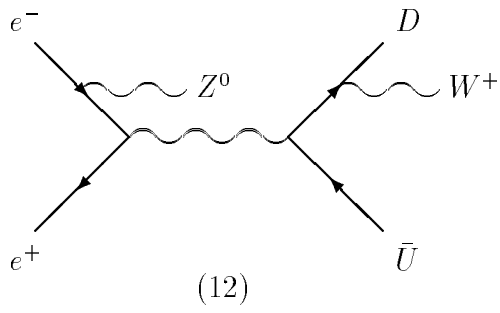
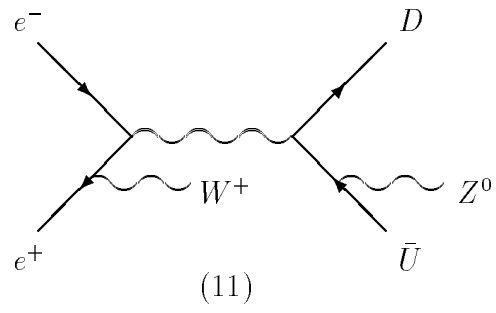
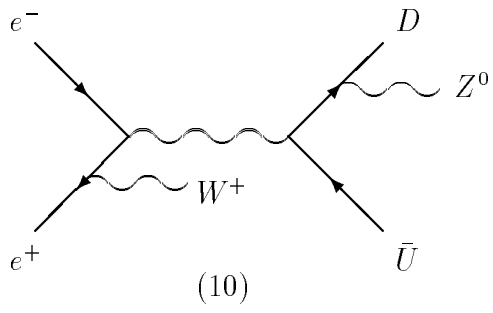


Fig. 1b (Continued)

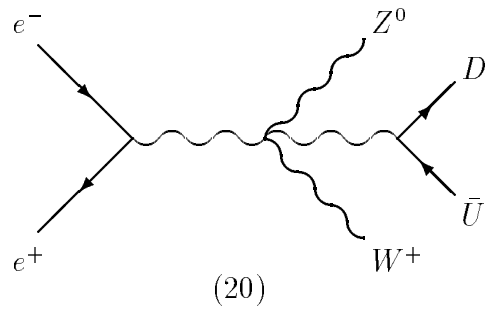
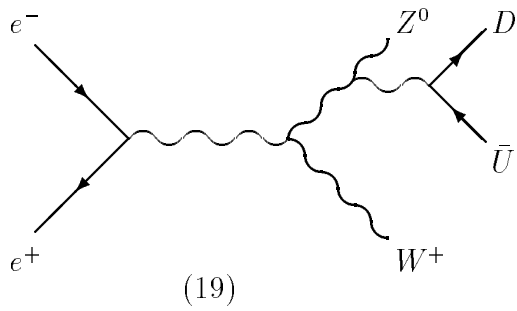
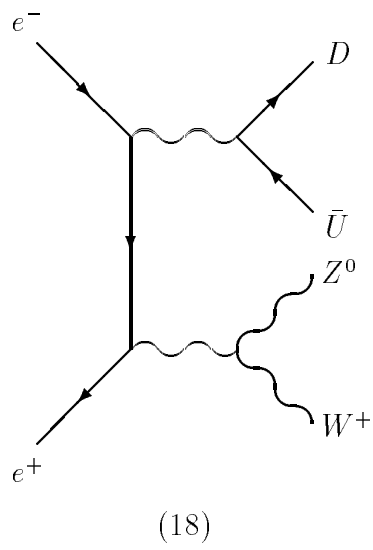
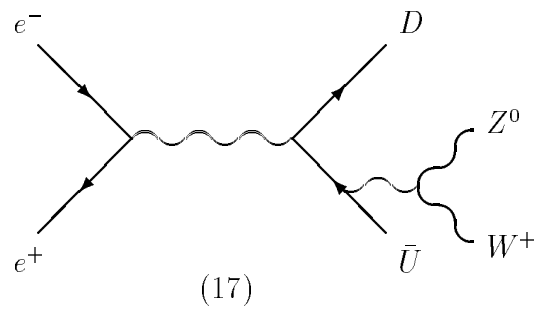
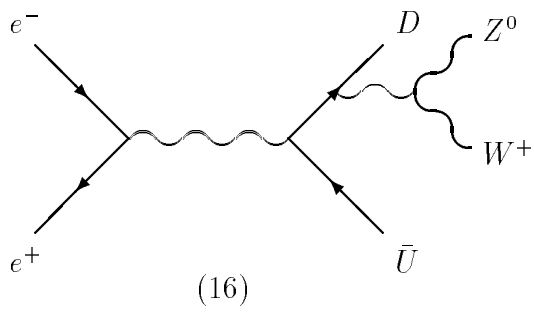


Fig. 1b (Continued)

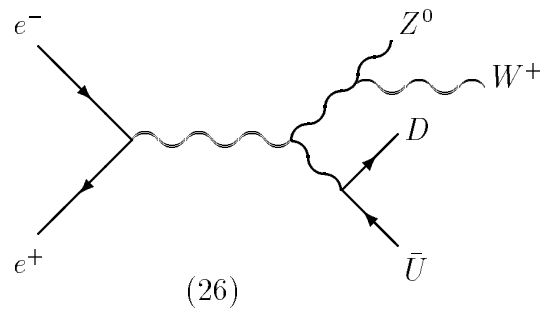
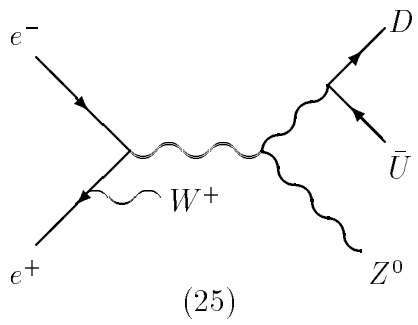
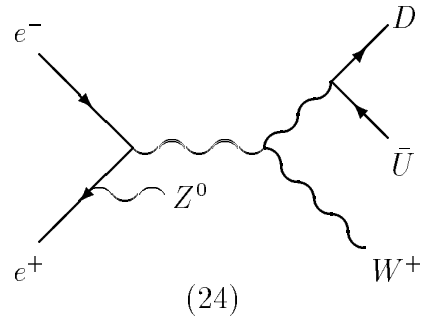
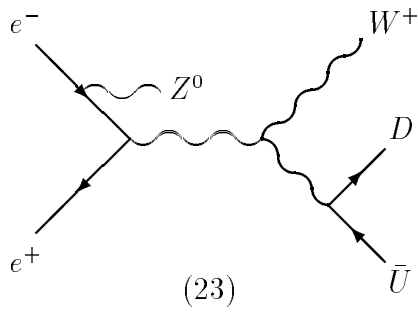
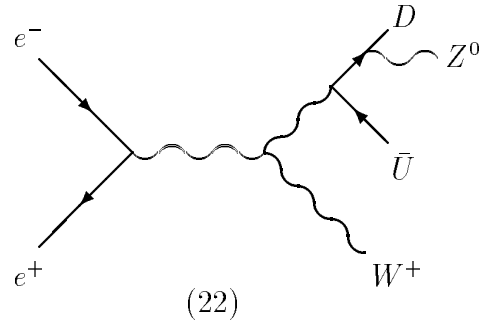
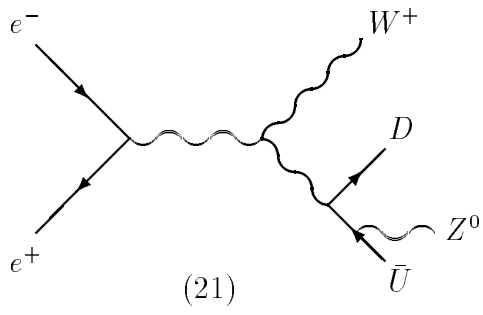


Fig. 1b (Continued)

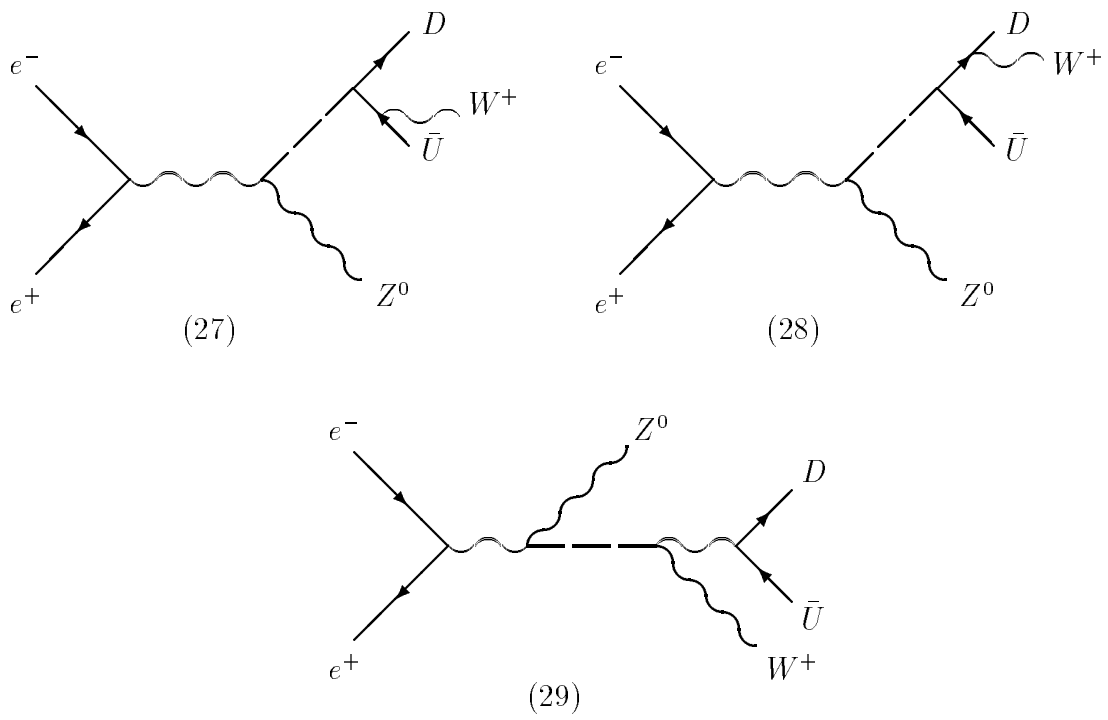


Fig. 1b (Continued)

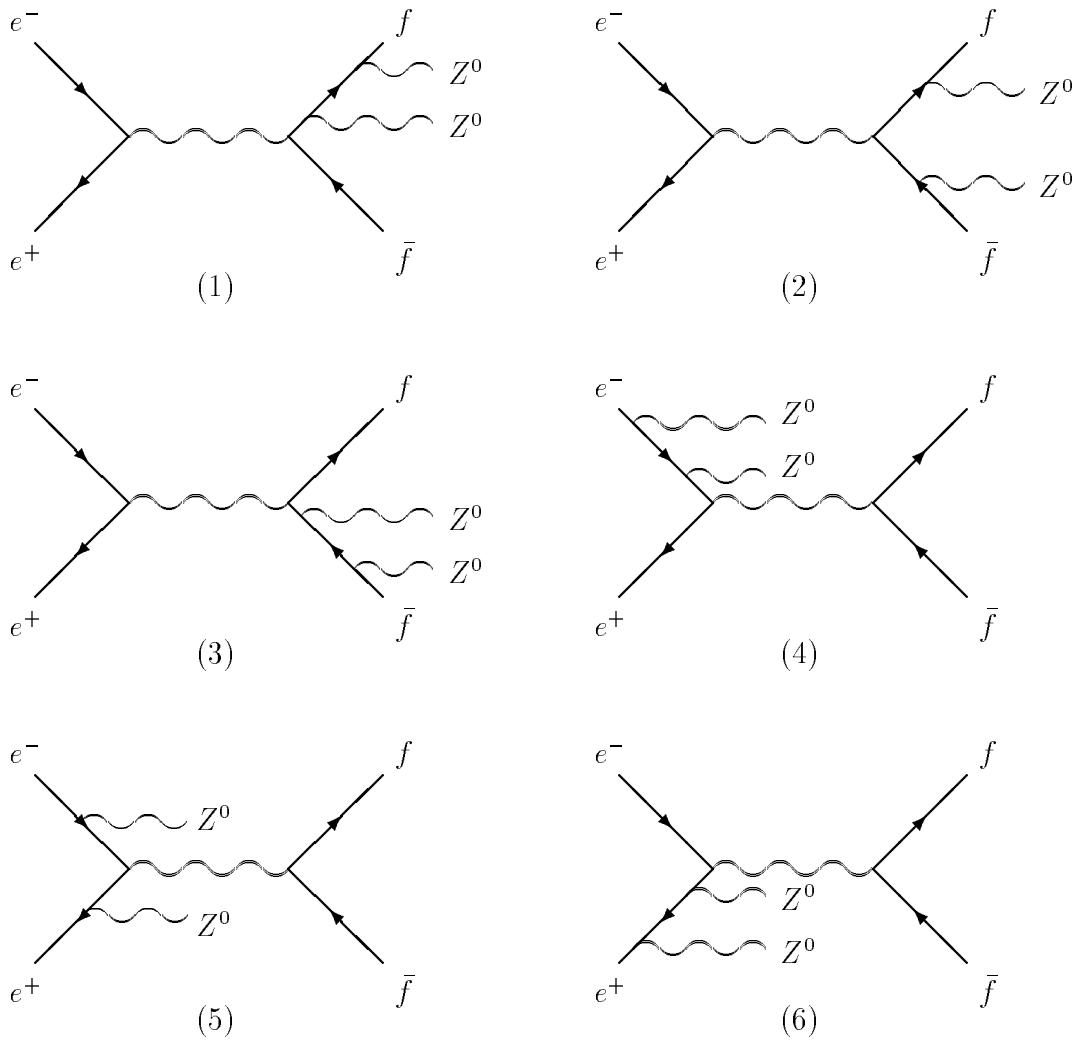


Fig. 1c

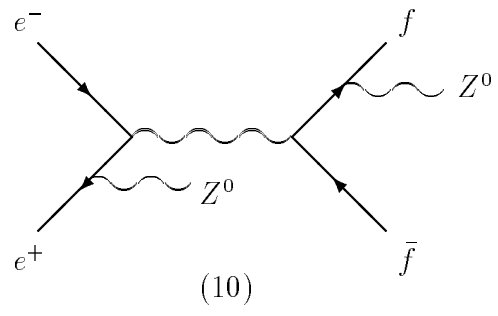
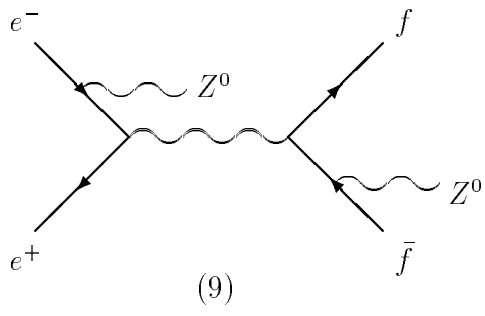
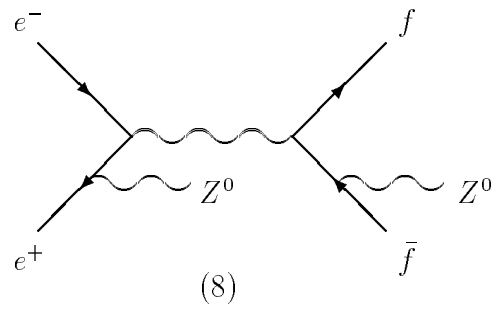
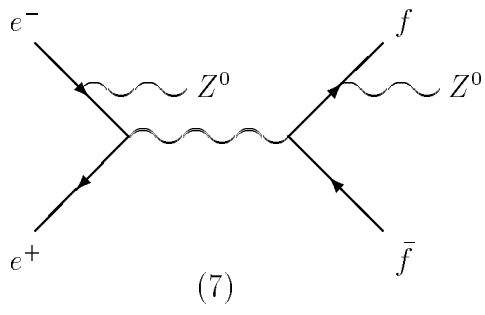


Fig. 1c (Continued)

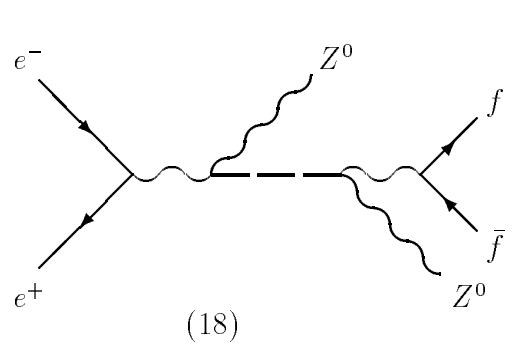
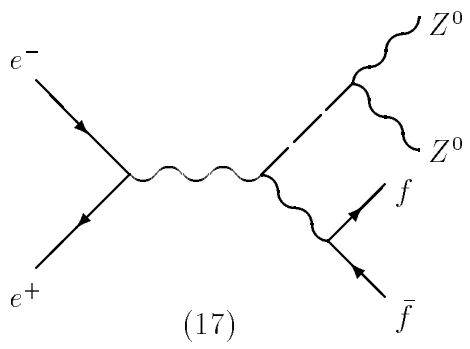
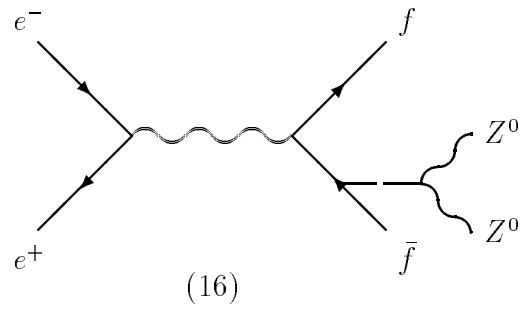
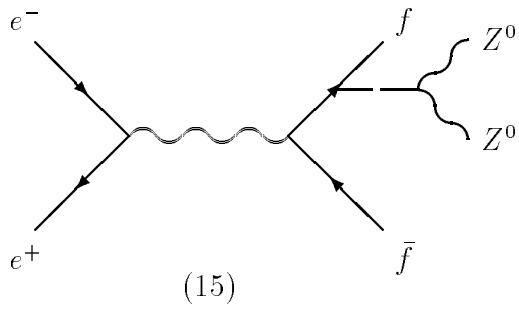
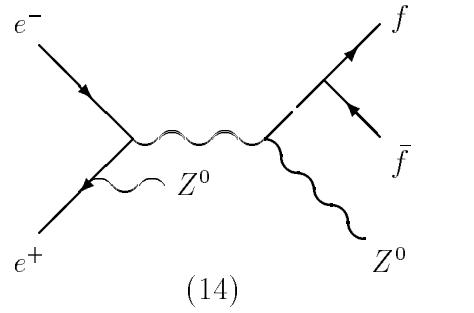
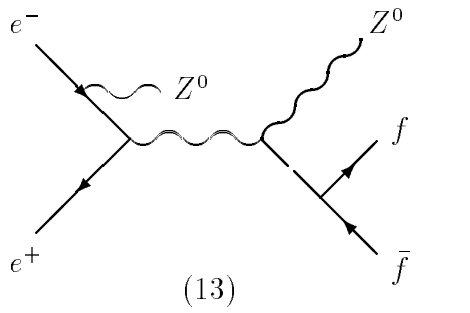
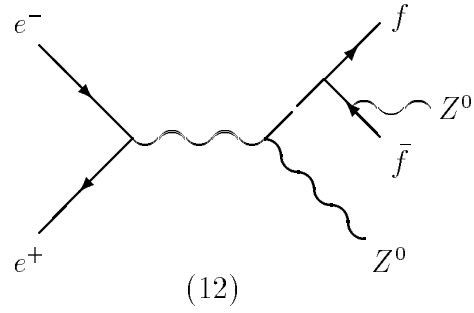
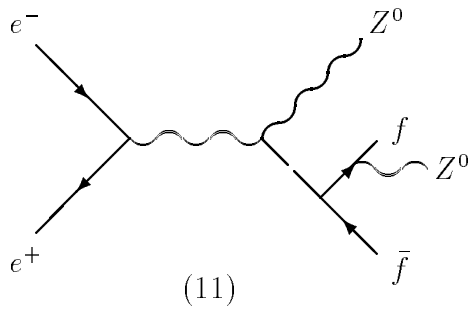


Fig. 1c (Continued)

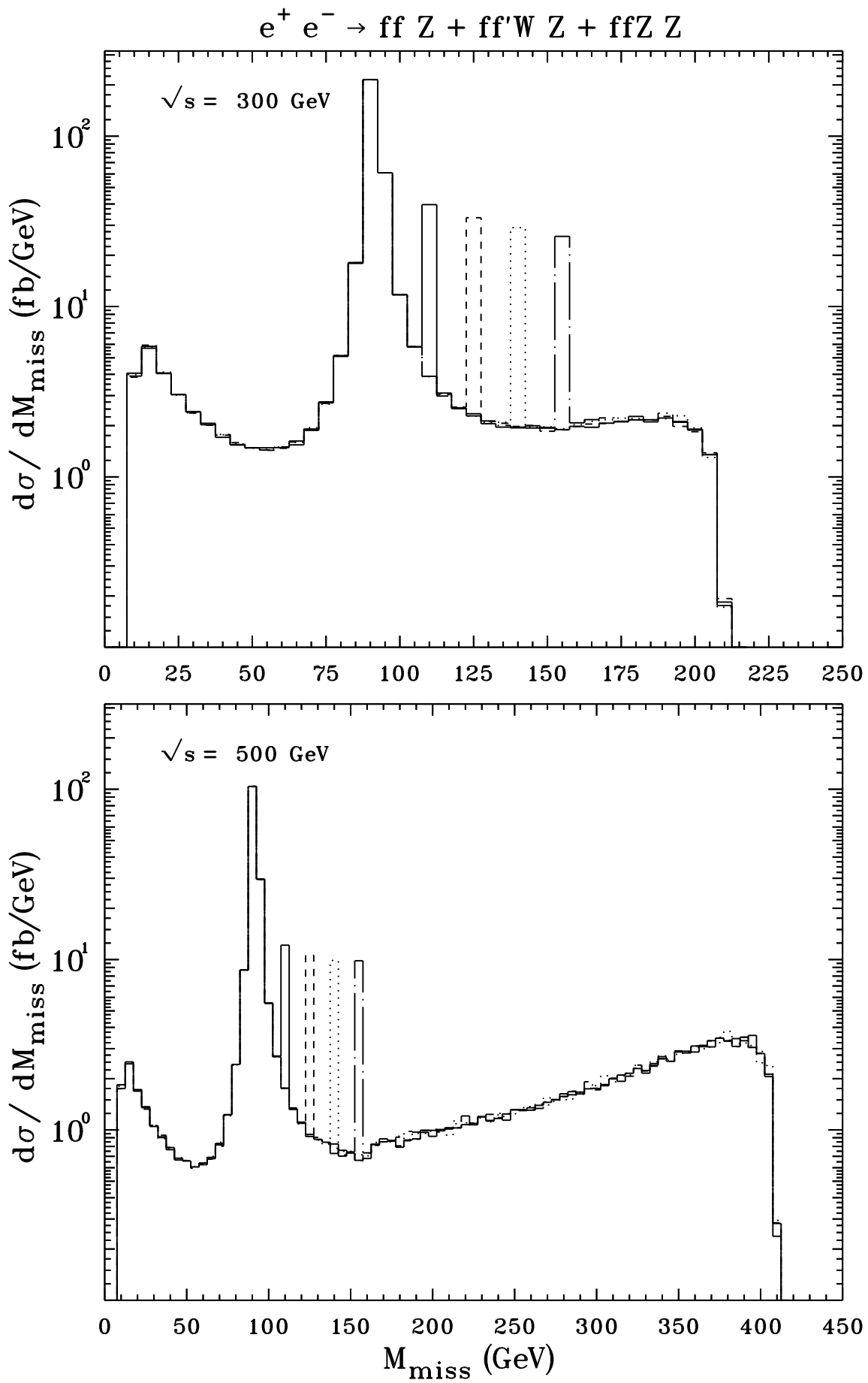


Fig. 2

$$e^+ e^- \rightarrow ff Z + ff'W Z + ffZ Z$$

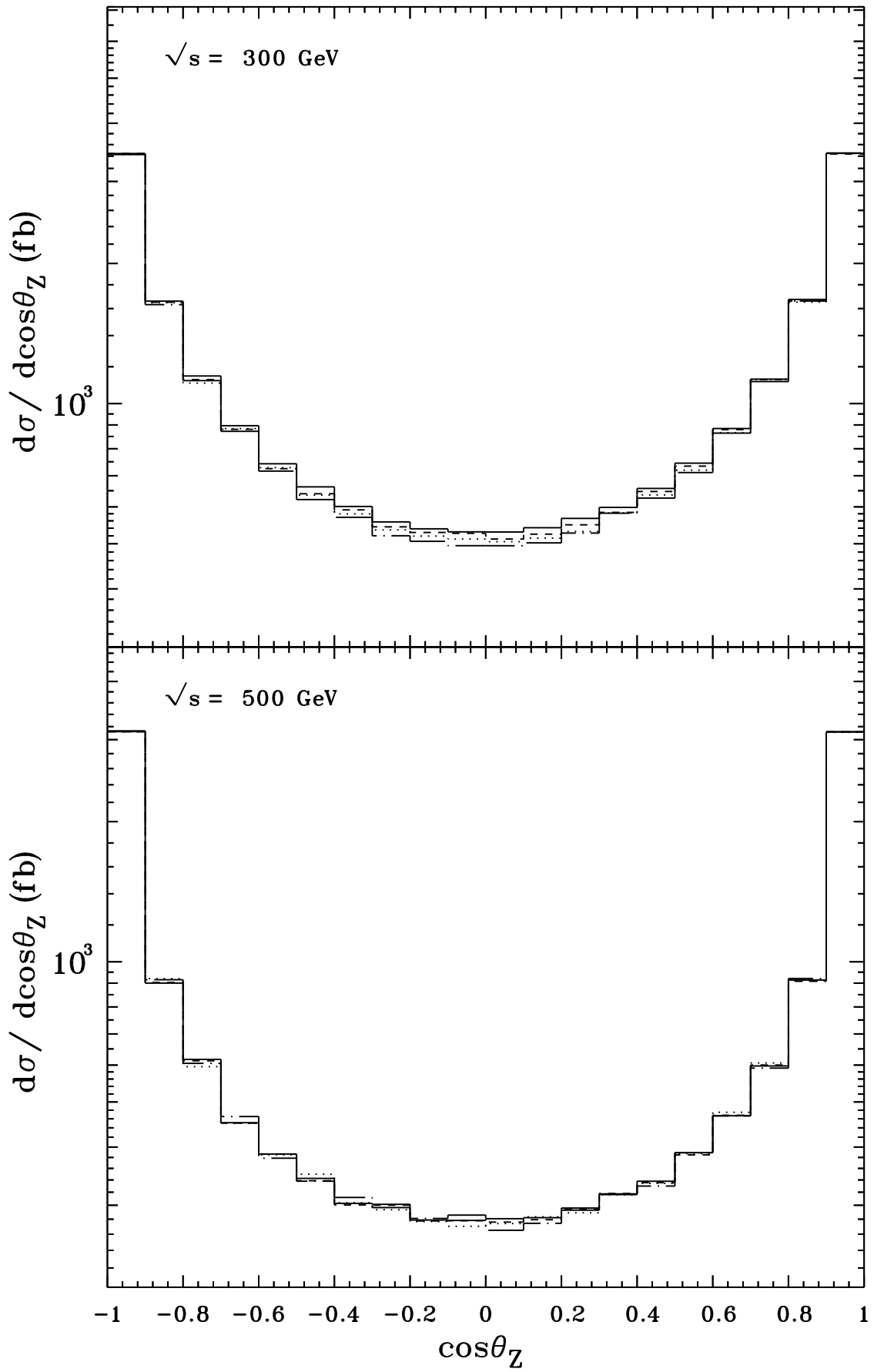


Fig. 3

$$e^+ e^- \rightarrow ff Z + ff'W Z + ffZ Z$$

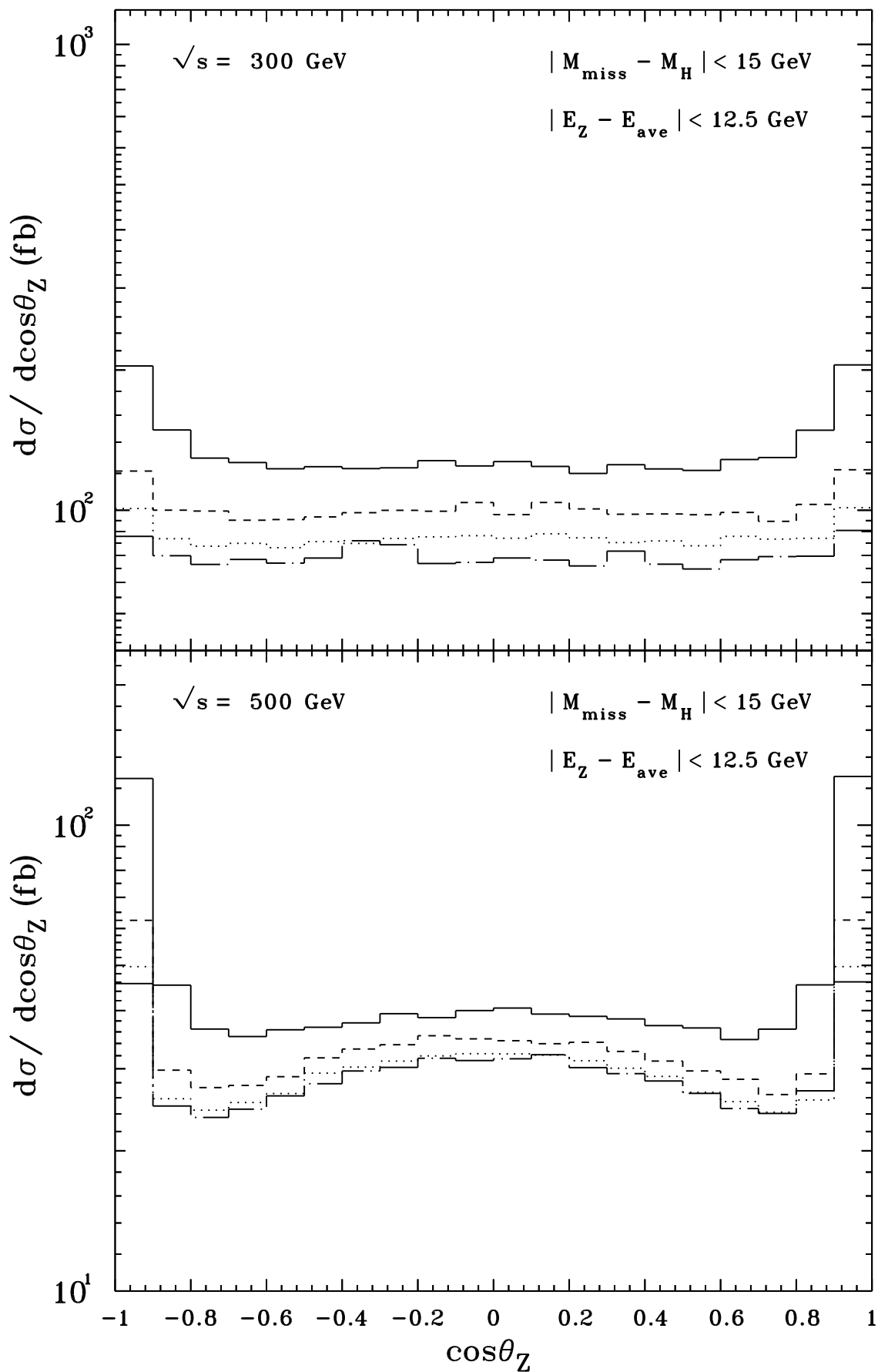


Fig. 4